2021 Joint International EUROSOI Workshop and International Conference on Ultimate Integration on Silicon (EuroSOI-ULIS) | 978-1-6654-3745-5/21/$31.00 ©2021 IEEE | DOI: 10.1109/EuroSOI-ULIS53016.2021.9560183

First Principles Evaluation of Topologically Protected Edge States in MoS_2 1T′ Nanoribbons with Realistic Terminations

Al-Moatasem El-Sayed
Institute for Microelectronics
Technical University of Vienna
Vienna, Austria, and
Nanolayers Research Computing Ltd.
1 Granville Court
London, U.K.
elsayed@iue.tuwien.ac.at

Heribert Seiler
Institute for Microelectronics
Technical University of Vienna
Vienna, Austria
seiler@iue.tuwien.ac.at

Hans Kosina
Institute for Microelectronics
Technical University of Vienna
Vienna, Austria
kosina@iue.tuwien.ac.at

Markus Jech
Institute for Microelectronics
Technical University of Vienna
Vienna, Austria
jech@iue.tuwien.ac.at

Dominic Waldhör
Institute for Microelectronics
Technical University of Vienna
Vienna, Austria
waldhoer@iue.tuwien.ac.at

Viktor Sverdlov
Christian Doppler Laboratory for
Nonvolatile Magnetoresistive Memory and Logic
at the Institute for Microelectronics
Technical University of Vienna
Vienna, Austria
sverdlov@iue.tuwien.ac.at

***Abstract*—Exploiting novel materials with advanced properties is necessary to improve device performance and continue with their scaling for high performance applications at reduced power. Among these materials, topological insulators (TIs) present an exciting opportunity where the highly conductive edge states, which are protected against back scattering, can lead to advances in electronic as well as spin controlled devices. Here, we present first principles results that evaluate topologically protected edge states in MoS_2 nanoribbons. We vary the width of the nanoribbons and show that they transition to trivial insulators below a critical width. Furthermore, the trivial insulator can be a direct or indirect band gap insulator depending on the width and the edge termination. Our results show that including realistic edge terminations can provide valuable insight, especially for narrow width TIs.**

***Index Terms*—Density Functional Theory, Edge States, Topological Insulators, Nanoribbons**

I. Introduction

Over the past decade, well-known two-dimensional transition metal dichalcogenides (TMDs) – such as MoS_2, $MoSe_2$, WS_2, and WSe_2 – have been shown to exist in topologically non-trivial phases known synonymously as either TIs or quantum spin hall insulators [1]–[5]. This behavior does not occur in their 2H polymorph, which is their ground state, but rather in other high energy polymorphs including the 1T′ phase. Their topological nature stems from the underlying symmetries that their Hamiltonians possess, which leads to their electronic structure being classified by a robust $\mathbb{Z}_2$ invariant of 1, whereas that of a trivial insulator is 0 [6]. As a necessary consequence of their non-trivial topology, interfacing them with a trivial insulator results in chiral, zero gap edge states with outstanding properties including linear dispersion, spin-momentum locking, and resistance to back-scattering [6], [7]. Reliably understanding their behavior is expected to bring about exciting advances in electronic and spintronic devices.

Studies in the literature have used both *ab initio* and semi-empirical methods to describe the electronic structure of the different 1T′ TMDs. Various $\mathbf{k} \cdot \mathbf{p}$ and tight-binding model Hamiltonians whose parameters were fitted to the bulk dispersion relations have been used to predict the behavior of the topologically protected edge modes in nanoribbons [1], [3], [4], [8]. At small nanoribbon widths, due to an interaction of the topologically protected states from the opposite edges in a nanoribbon, a small gap in the otherwise gapless linear spectrum of the edge states is predicted to open [8]. This results in a decrease of the ballistic conductance compared to a semi-infinite sample. This gap increases when an electric field is applied perpendicular to the nanoribbon resulting in a further reduction of the conductance. At the same time the separation between the bulk bands decreases with the orthogonal field. The edge-localized modes transform into the bulk-like modes when their dispersion intersect, signifying a transition from a TI to a trivial insulator. As no edge modes protected from back-scattering exist at higher electric fields, the conductance decreases dramatically [9]. Studies using *ab initio* and tight-binding calculations also show that a gap opens in the edge states [4], [5], [10]. However, these studies additionally show that the electronic structure of these narrow nanoribbons are highly dependent on the reconstruction of the edges' atomic

structure.

Here, we use density functional theory (DFT) to model monolayer and realistic terminations of narrow nanoribbons of MoS_2 1T′. We focus on nanoribbons cleaved in the y-direction, such as the terminations shown in Fig. 1, in contrast to previous studies in the literature which studied nanoribbons cleaved in the x-direction [5], [10]. We show that at small widths, the nanoribbons no longer have edge states in the band gap. This is in contrast to nanoribbons cleaved in the x-direction which possess gapless edge states even at relatively small widths. Furthermore, we show that depending on the termination, the electronic structure transitions to an indirect band gap.

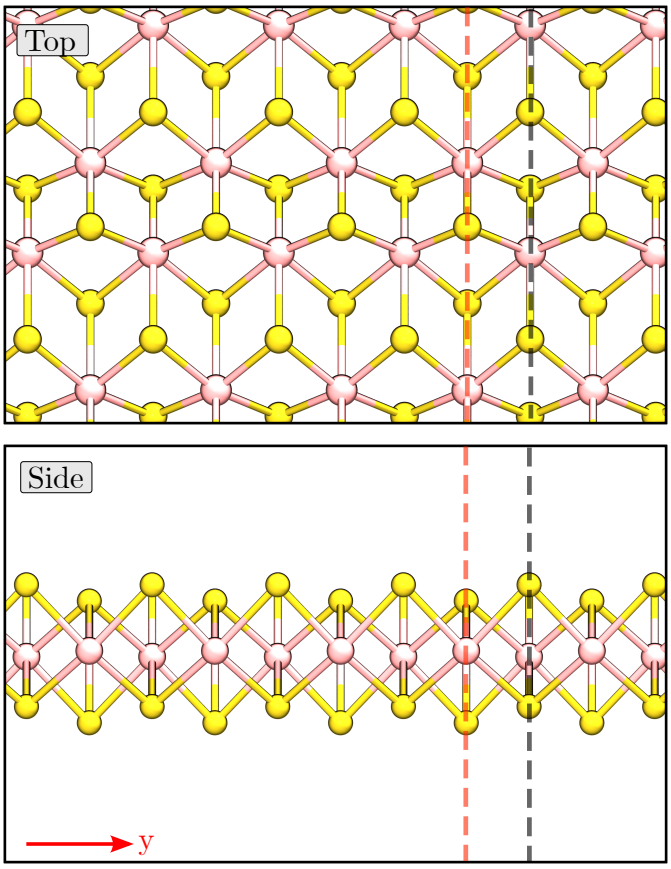

Fig. 1. The MoS_2 1T′ structure from the top and the side. The black and red dashed lines indicate the two possible, chemically equivalent, terminations along the y-direction and are made along the same plane for both top and side views. The red arrow in the bottom panel indicates the direction of the y-axis for both the top and side views. The pink spheres are the Mo atoms while the yellow spheres are S atoms.

II. Methods

We use DFT as implemented in the Vienna Ab-Initio Simulation Package (VASP) to calculate both monolayer and nanoribbon systems of MoS_2 1T′. Exchange and correlation were described using the generalized gradient Perdew-Burke-Ernzerhof (PBE) functional [11]. The projector augmented wave method and its associated pseudopotentials were used in all calculations. The electron density was expanded in a plane wave basis set whose cutoff was set to 280 eV. The system's k-space was sampled on a Monkhorst pack grid of $8 \times 1 \times 1$ for geometry optimizations and $12 \times 1 \times 1$ for band structure calculations of the nanoribbons. For the bulk monolayer, this changes to $8 \times 8 \times 1$ for geometry optimizations and $12 \times 12 \times 1$ for band structure calculations. Electron densities were converged until the energy change was less than 10^{-4} eV. Geometries were optimized so that the energy changed by less than 10^{-3} eV. The topological edge states of TMDs depend on the band gap opening due to a spin-orbit interaction; therefore, all band structure calculations include the spin-orbit coupling [12].

In this paper, we focus on the 1T′ structure of MoS_2. To model the bulk monolayer, a vacuum gap of 2 nm was included in the z- direction and the cell and its atomic coordinates were optimized. The nanoribbon structures were then created by introducing another vacuum gap of 2 nm in the y-direction. Thus, the only remaining periodic dimension is the x-direction. After introduction of the vacuum gap, the atomic structure of the nanoribbons were optimized once more, resulting in significant reorganization of the edges which we refer to as realistic terminations.

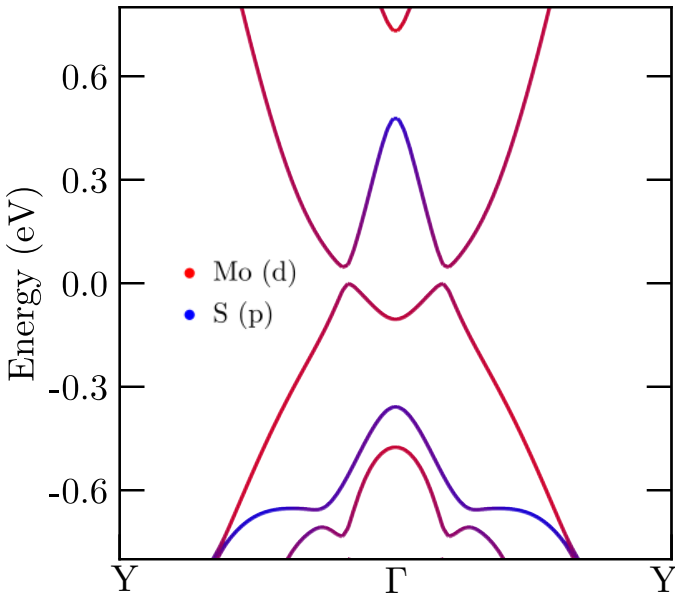

Fig. 2. Band structure of a monolayer of MoS_2 1T′. The band structure is projected onto the Mo 'd' states (red) and S 'p' states (blue).

III. Results

We start by calculating the band structure of a monolayer of MoS_2 1T′. Using a single unit cell containing six atoms, the cell and its atomic coordinates were optimized and the electronic structure was calculated. Fig. 1 shows the optimized atomic structure which is replicated for ease of visualization. The optimized 1T′ structure has Mo–S bond lengths of 2.39, 2.48, and 2.51 Å. The band structure of the system can be seen in Fig. 2 and has been projected onto the Mo 'd' and S 'p' orbitals. Around the Fermi level, which is at 0 eV, a

band gap of 0.08 eV appears due to the spin-orbit coupling. Without it, the system would be a semi-metal. In addition, an inverted band gap of 0.56 eV appears where the conduction band is mostly made of S 'p' orbitals and the valence band is made of Mo 'd' orbitals. This is in good agreement with what has been reported in the literature and the inverted band gap as well as the spin-orbit band gap are qualitatively what one would expect from a TI [1], [3]. The $\mathbb{Z}_2$ invariant can be numerically calculated as implemented in the Z2pack code and indeed the $\mathbb{Z}_2$ of the MoS_2 1T′ was found to be 1 [13].

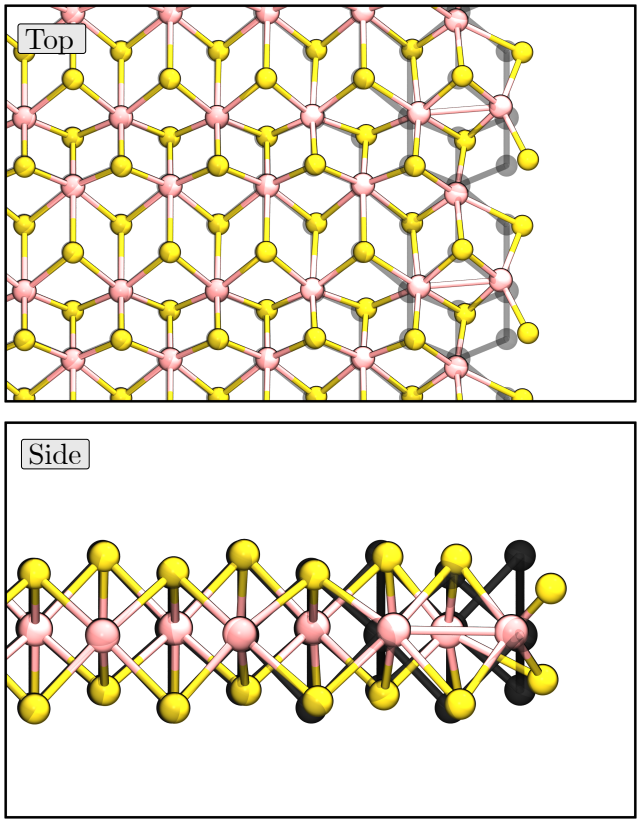

Fig. 3. A nanoribbon of MoS_2 1T′ cleaved along the y-direction. The coloured atomic system is the geometry optimized structure, while the black, transparent system is the initial, unrelaxed structure. The color scheme is the same as in Fig. 1

We now turn our attention to nanoribbons of MoS_2 1T′ cleaved along the y-direction. Cleaving the MoS_2 sheet results in two structural edges. Although they are chemically equivalent, they lead to two possible combinations. When both structural edge types are the same, we refer to this as symmetric, and when they are different they are asymmetric as depicted in Fig. 1. We modeled three different nanoribbon widths: 1.2 nm, 3.8 nm, and 7.9 nm. For all widths, the edges were cleaved and the structure was optimized, leading to reorganization of the edge atoms. The behavior of the relaxation was qualitatively the same regardless of nanotube width and the type of edge termination. The optimization is indicated in Fig. 3, where it is also compared to the initial, unrelaxed structure. The edge can be found on the right side of the figure, where the strongest atomic displacement occurs. One immediately sees that the displacements only persist over four to five layers of the nanoribbon. The Mo atoms at the edge tend to displace toward the nanoribbon while the S atoms displace away from the nanoribbon. Optimizing the nanoribbon does not introduce a net magnetic moment which would break time reversal symmetry and thus one of the underlying symmetries required for the topologically protected edge states. Conflicting *ab initio* calculations of the magnetic moment do not agree whether nanoribbons cleaved along the x-direction possess a magnetic moment [5], [10].

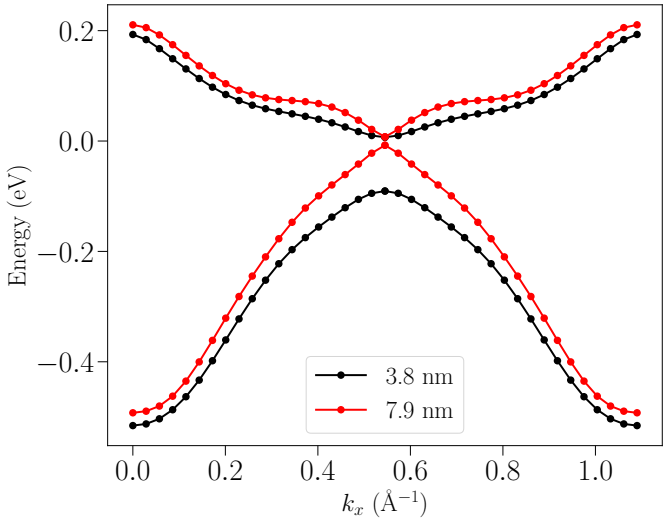

Fig. 4. The highest occupied and lowest occupied bands of two nanoribbon widths of MoS_2 1T′. The narrower, 3.8 nm, nanoribbon's bands are shown in black, while the wider, 7.9 nm, nanoribbon's bands are shown in red. One can see the linear dispersion of the edge states in the wide nanoribbon.

The electronic structure of the nanoribbons was calculated and varies with the width of the nanoribbon. The first thing to note is the appearance of a gap in the topologically protected edge states. This can be seen in Fig. 4, which shows the highest occupied and lowest unoccupied bands of two nanoribbons of different widths. The wider nanoribbon, 7.9 nm, shows linear dispersion of gapless states around the Fermi level at 0 eV, typically associated with the topologically protected edge states. As the width is reduced to 3.8 nm, the states are no longer linearly dispersed and appear to become more parabolic. This behavior was the same regardless whether the edge was symmetrically or asymmetrically terminated. In addition, a band gap of 0.1 eV appears between these edge states. Similar effects have also been seen in MoS_2 1T′ nanoribbons that were cleaved in the x-direction [5], [10]. However, in that case, the gap only appeared at widths less than 2 nm and their magnitude was typically much smaller than the gap shown here for nanoribbons cleaved in the y-direction. In addition, *ab initio* calculations showed that of the six possible terminations, only two supported edge states without any other surface states [10]. However, on the y-axis edge, the topological edge states can be seen regardless of the

termination.

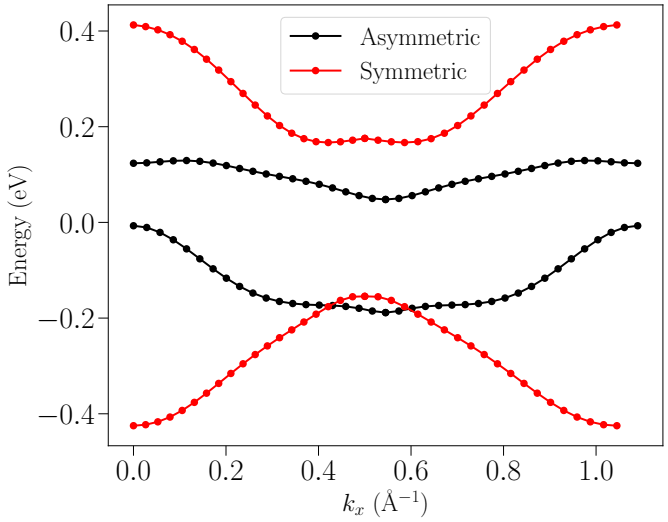

Fig. 5. The highest occupied and lowest occupied bands of two nanoribbon widths of a 1.2 nm strip of MoS_2 1T′. The bands of the asymmetric termination are shown in black while those of the symmetric termination are red. The Γ point of the reciprocal cell occurs at a k_x value of 0.54 Å^{-1}.

For narrow nanoribbons, the qualitative behavior changes depending on the termination. Fig. 5 shows the highest occupied and lowest unoccupied bands of a 1.2 nm wide nanoribbon terminated either symmetrically or asymmetrically as depicted in Fig. 1. Due to the narrow width of the nanoribbon and the interaction between the edge states, a large band gap opens up for both terminations. For the symmetric termination, the band gap is 0.3 eV, while it is 0.1 eV for the asymmetric termination. Curiously, for both terminations the qualitative nature of the edge state band gap changes from direct to indirect. For the symmetric nanoribbon, this is a slight shift, so that two minima appear in the conduction band which are shifted by 0.1 Å^{-1} from the valence band maximum. However, for the asymmetric termination, the lowest conduction band minimum is located at the Γ point while the valence band maximum is at the Brillouin zone edge, indicating that band to band transitions in the asymmetric narrow nanoribbons could be suppressed due to the large change in crystal momentum required.

Discussion and Conclusions

The highly conductive topologically protected edge states of TIs can have a high impact on electronic devices. However, many fundamental models and theories are based on the properties of the bulk Hamiltonian and ignore the potential changes in the Hamiltonian for downsized systems as well as the effect of edge reorganization. Here, we have calculated the electronic structure of nanoribbons of topologically insulating MoS_2 1T′ where the width of the nanoribbon was less than 8 nm. One can see that the edge states begin to interact with each other below 4 nm to open a band gap. This could indicate that some of the fundamental symmetries required for a topologically protected zero energy state have been broken. This effect, although still disputed, occurs for nanoribbons of MoS_2 1T′ cleaved in the x-direction, where the introduction of certain edges introduce a magnetic moment which would break time-reversal symmetry, an essential component of the non-trivial $\mathbb{Z}_2$ invariant [5], [14]. However, our calculations show that edges along the y-direction do not possess a magnetic moment. Furthermore, our results show that the edge termination can have a strong quantitative and qualitative effect on very narrow nanoribbons of MoS_2 1T′.

Acknowledgment

The financial support by the Austrian Federal Ministry for Digital and Economic Affairs, the National Foundation for Research, Technology and Development and the Christian Doppler Research Association is gratefully acknowledged. The authors are grateful for the support from the Vienna Scientific Cluster, who provided computer resources on the Austrian high-performance clusters VSC3 and VSC4.

References

[1] Q. Xiaofeng, L. Junwei, F. Liang, and L. Ju, "Quantum spin Hall effect in two-dimensional transition metal dichalcogenides," *Science*, vol. 346, no. 6215, pp. 1344–1348, 2014.

[2] T. Olsen, "Designing in-plane heterostructures of quantum spin Hall insulators from first principles: 1T′-MoS2 with adsorbates," *Phys. Rev. B*, vol. 235106, no. 23, pp. 1–9, 2016.

[3] B. Das, D. Sen, and S. Mahapatra, "Tuneable quantum spin Hall states in confined 1T′ transition metal dichalcogenides," *Sci. Rep.*, vol. 10, no. 1, pp. 1–13, 2020.

[4] A. Lau, R. Ray, D. Varjas, and A. R. Akhmerov, "Influence of lattice termination on the edge states of the quantum spin Hall insulator monolayer 1T′-WTe2," *Phys. Rev. Mater.*, vol. 3, no. 5, pp. 1–9, 2019.

[5] L. Jelver, D. Stradi, K. Stokbro, T. Olsen, and K. W. Jacobsen, "Spontaneous breaking of time-reversal symmetry at the edges of 1T′ monolayer transition metal dichalcogenides," *Phys. Rev. B*, vol. 99, no. 15, p. 155420, 2019. [Online]. Available: https://doi.org/10.1103/PhysRevB.99.155420

[6] M. Z. Hasan and C. L. Kane, "Colloquium: Topological insulators," *Rev. Mod. Phys.*, vol. 82, no. 4, pp. 3045–3067, 2010.

[7] X. L. Qi and S. C. Zhang, "Topological insulators and superconductors," *Rev. Mod. Phys.*, vol. 83, no. 4, 2011.

[8] V. Sverdlov, A. M. B. El-Sayed, H. Kosina, and S. Selberherr, "Conductance in a Nanoribbon of Topologically Insulating MoS_2 in the 1T′ Phase," *IEEE Trans. Electron Devices*, vol. 67, no. 11, pp. 4687–4690, 2020.

[9] B. Zhou, H. Z. Lu, R. L. Chu, S. Q. Shen, and Q. Niu, "Finite size effects on helical edge states in a quantum spin-hall system," *Phys. Rev. Lett.*, vol. 101, no. 24, pp. 1–4, 2008.

[10] A. Pulkin and O. V. Yazyev, "Controlling the Quantum Spin Hall Edge States in Two-Dimensional Transition Metal Dichalcogenides," *J. Phys. Chem. Lett.*, vol. 11, no. 17, pp. 6964–6969, 2020.

[11] J. P. Perdew, K. Burke, and Y. Wang, "Generalized gradient approximation for the exchange-correlation hole of a many-electron system," *Phys. Rev. B*, vol. 54, no. 23, pp. 16 533–16 539, dec 1996. [Online]. Available: http://www.tandfonline.com/doi/abs/10.1080/13639080.2012.711944 https://link.aps.org/doi/10.1103/PhysRevB.54.16533

[12] E. v. Lenthe, E. J. Baerends, and J. G. Snijders, "Relativistic regular two-component hamiltonians," *J. Chem. Phys.*, vol. 99, no. 6, pp. 4597–4610, 1993. [Online]. Available: https://doi.org/10.1063/1.466059

[13] D. Gresch, G. Autès, O. V. Yazyev, M. Troyer, D. Vanderbilt, B. A. Bernevig, and A. A. Soluyanov, "Z2Pack: Numerical implementation of hybrid Wannier centers for identifying topological materials," *Phys. Rev. B*, vol. 95, no. 7, pp. 1–24, 2017.

[14] K. Chen, J. Deng, X. Ding, J. Sun, S. Yang, and J. Z. Liu, "Ferromagnetism of 1T′-MoS_2 Nanoribbons Stabilized by Edge Reconstruction and Its Periodic Variation on Nanoribbons Width," *J. Am. Chem. Soc.*, vol. 140, no. 47, pp. 16 206–16 212, 2018.